Application of a Radiative-Conductive Model to the Simulation of Nocturnal Temperature Changes over Different Soil Types

WILFORD G. ZDUNKOWSKI AND DAVID C. TRASK

Dept. of Meteorology, University of Utah, Salt Lake City

(Manuscript received 12 November 1970, in revised form 8 June 1971)

ABSTRACT

For a calm night, nocturnal temperature profiles pertaining to various soil types are computed for the entire boundary layer. The mathematical analysis is based upon a numerical solution of the equations of motion, heat conduction and radiative transfer. The effect of radiative temperature change upon the total cooling rate is investigated. Some other interesting quantities associated with the distribution of the exchange coefficient and wind velocity components as a function of height and time are also calculated.

Solutions are presented in graphical format. All results such as temperature profiles, inversion heights and wind spirals seem to be in reasonable agreement with theoretical and observational deductions.

1. Introduction

There are a number of investigations in the literature which deal with the prediction of the nocturnal temperature profile. No attempt is made here to review in detail the accomplishments of the past. However, it is relevant to this study to discuss briefly some of the more important papers on this subject.

The classical method of predicting the nocturnal temperature profile of the boundary layer is best exemplified by the approach taken by Philipps (1940). He assumes that initially the system earth-atmosphere is in the isothermal state. Regarding the net flux of longwave radiation at the surface of the earth as constant for the course of a night, disregarding altogether the radiative flux divergence of the air, assuming that the exchange coefficient of the air and the soil are constant, the problem presents itself in finding a solution to two linear heat conduction equations. Subject to certain boundary conditions, Phillipps was able to find an analytic solution by standard methods following more or less a procedure first outlined by Brunt (1940).

In the lower 2 m, as is well known now, the atmospheric exchange coefficient changes by a few orders of magnitude so that the assumption of a constant exchange coefficient must be abandoned. Moreover, the radiative net flux during a night may also change appreciably. For these reasons alone, it is no longer feasible to uphold the classical approach. Philipps (1962) improved his analysis by changing the initial conditions and by approximately including the effects of advection. He retained the assumption of a constant air exchange coefficient.

Jaeger (1945) and Knighting (1950) make the improved assumption that the exchange coefficient changes according to a power law in which the height coordinate is raised to a power. The exponent, presumably a function of the stability of the air, is held constant in the analysis. The choice of the constants involved in the power law is arbitrary and therefore not well suited for practical purposes. Their radiation treatment parallels that of Philipps (1940).

A new and much more promising approach to the problem of the nocturnal temperature prediction is due to Gaevskaya *et al.* (1962). These authors take into account, in an approximate manner, the effects of the radiative flux divergence of the air, and more importantly, the variation of the exchange coefficient with height in a prearranged manner. No allowance is made for the variation of the exchange coefficient with time. The self-criticism of these authors is highly significant. They state: "The present formulation of the problem is not logically complete since the coefficient of turbulent mixing is introduced as an external parameter, independent of temperature and wind distribution."

Zdunkowski *et al.* (1967) predict the nocturnal temperature profile by a method similar to that outlined by Gaevskaya *et al.* Their analysis, however, is based upon a more realistic formulation of the exchange coefficient of the air which takes into account, although in a somewhat crude manner, the effect of stability.

A very ingeneous and fairly complete analysis of the diurnal temperature profile is due to Kuo (1968). In order to obtain usable analytic solutions, he introduces a simplified radiation treatment by dividing the absorption spectrum of terrestrial radiation into strongly and weakly absorbing regions. Such a simplification is compatible with various other approximation made in that

paper. Although Kuo's type of analysis is very useful in studying interactions of various processes, it is not so well adapted in predicting the nocturnal temperature regime.

Some pioneering work of modelling the boundary layer is due to Estoque (1963) whose work is extended by Pandolfo et al. (1964, 1965). Their analyses are based upon the assumption of a constant flux layer. Kuo (1968), however, comes to the conclusion that such a model is not capable of adequately representing the temperature variation in the thermal boundary layer.

It is the opinion of the authors of the present paper that it is not possible to reliably predict the nocturnal temperature profile by existing analytic solutions. Moreover, it presently seems hopeless to extend these solutions to incorporate satisfactorily the variations of the exchange coefficient and the effects of radiative flux divergence. Therefore, the solution to the problem is best found in terms of numerical techniques.

It is the aim of this paper to remove previously mentioned shortcomings to some extent and to predict the nocturnal temperature profile near the ground on a fairly realistic physical basis. The variation of the net flux at the ground as a function of time as well as the radiative flux divergence of the air are accounted for. The effects of stability on the height-dependent exchange coefficient are considered by generating internally the exchange coefficient for a given set of initial conditions and non-changing physical parameters such as roughness height and latitude. It is only necessary to make plausible assumptions as to the mathematical form of the mixing length. As *additional* information, the distribution of the exchange coefficients and wind spirals are obtained. It appears that all computed quantities are physically realistic.

2. Mathematical analysis

a. Basic relationships[1]

It is assumed that the basic equations describing the temperature distribution of the lower part of the atmosphere and the upper soil layer in a calm fog and cloud-free night are given by

$$\frac{\partial\theta}{\partial t}=\frac{\partial}{\partial z}\left(K_H\frac{\partial\theta}{\partial z}\right)=-\frac{1}{\rho c_p}\frac{\partial F_N}{\partial z}\left(\frac{1000}{p}\right)^{\varkappa},\quad z>0,\ t>0, \tag{1a}$$

$$\frac{\partial T_s}{\partial t}=\frac{\partial}{\partial z}\left(K_s\frac{\partial T_s}{\partial z}\right),\qquad z<0,\ t>0. \tag{1b}$$

Initial conditions needed to solve this system of equations pertain to data at the time of sundown, the starting time of the prediction analysis. The proper boundary condition at the air-soil interface and conditions at infinity are given as

$$\left.\begin{aligned}&-F_N+c_p\rho K_H\frac{\partial\theta}{\partial z}-\rho_s c_s K_s\frac{\partial T_s}{\partial z}=0,\quad z=0,\ t>0\\ &\left.\begin{aligned}T_{\text{Air}}&=T_s, && z=0\\ \theta&=\text{constant}, && z=\infty\\ T_s&=\text{constant}, && z=-\infty\end{aligned}\right\},\quad t\gtrless 0.\end{aligned}\right\} \tag{1c}$$

b. Radiation computations

In order to carry out the analysis in an efficient manner, all radiation computations use transmission functions free from wavelength. Such transmission data can be obtained from radiation charts or from free-air measurements. For boundary layer computations the temperature dependency of the transmission function can be disregarded. Since water vapor is the only radiatively active gas considered in this study, the net flux at the ground as required by Eq. (1c) is simply given by

$$F_N(z=0)=B(z=0)+\int_{\tau(w=0)}^{\tau(W)}B\,d\tau(w), \tag{2}$$

where W represents the total water vapor path length of the atmosphere.

The radiative temperature change at reference height z' as required for the evaluation of (1a) is computed by means of a differential method using the equation

$$\frac{\partial F_N(z')}{\partial z'}=-\int_{B(z=0)}^{B(z=\infty)}\frac{\partial\tau(w)}{\partial z'}dB+\left[\frac{B\partial\tau(w)}{\partial z'}\right]_{z=\infty},$$

where

$$\frac{\partial\tau}{\partial z'}=\frac{\partial\tau}{\partial w}\frac{dw}{dz'}. \tag{3}$$

It should be noted that $\partial\tau/\partial z'>0$ for $z>z'$ and $\partial\tau/\partial z'<0$ for $z<z'$. For details see Zdunkowski and Johnson (1965). As shown by Zdunkowski and Johnson it makes little consequence whether temperature changes near the ground are computed using either Möller's (1943) or Kuhn's (1963) radiation data.

Möller's (1943) transmission function is known to give reasonably accurate values of the downward flux at the ground. Therefore, his transmission data are used throughout this study. The inclusion of CO_2 effects can be accomplished without particular difficulties. Final results, however, show little effect at the expense of moderately large increases in computer costs.

c. The formulation of the exchange coefficient of air

The literature proposes a number of semi-empirical formulas to describe the distribution of the exchange

[1] A list of the more important symbols is given in Appendix A.

coefficient of the air layer near the ground under stable conditions. Since the distribution of the exchange coefficient for the entire boundary layer is required, the above-mentioned equations cannot be used.

Blackadar (1962), in formulating the exchange coefficient K_m for the entire neutrally stratified boundary layer, relies entirely on Heisenberg's (1948) hypothesis of energy dissipation ϵ which relates K_m and the mixing length such that

$$K_m=\epsilon^{\frac{1}{3}}l^{\frac{4}{3}}. \tag{4}$$

Denoting neutral conditions by the suffix n and using the relationships

$$\epsilon_n=K_{m,n}\left[\left(\frac{\partial u}{\partial z}\right)^2+\left(\frac{\partial v}{\partial z}\right)^2\right], \tag{5}$$

$$l=kz(1+kz/\lambda)^{-1}, \tag{6}$$

where λ is some relevant parameter, Blackadar (1962) obtains as a general statement for the exchange coefficient

$$K_{m,n}=\left[\left(\frac{\partial u}{\partial z}\right)^2+\left(\frac{\partial v}{\partial z}\right)^2\right]^{\frac{1}{2}}[kz/(1+kz/\lambda)]^2. \tag{7}$$

The advantage of (6) is that over small heights l increases linearly with height and that it approaches a fixed value at greater heights. This type of variation of mixing length is in harmony with numerous observations. Wu (1965) generalizes Eq. (7) by including the stability function

$$f(\theta)=\frac{gr}{T}\frac{\partial\theta}{\partial z}, \tag{8}$$

where r is a stability parameter defined by $K_H=rK_m$. Since the coefficient K_H, even under the most severe stability, cannot become less than the molecular diffusion coefficient K_{Mol}, the exchange coefficient for a non-neutral atmosphere can be written as

$$K_H=r\left[\left(\frac{\partial u}{\partial z}\right)^2+\left(\frac{\partial v}{\partial z}\right)^2-f(\theta)\right]^{\frac{1}{2}}\times[kz/(1+kz/\lambda)]^2+K_{\text{Mol}}. \tag{9}$$

It is this form of the exchange coefficient which is used throughout this study. Undoubtedly, λ is some function of stability. Attempts to specify variations of λ in terms of Richardson's number have failed. Very consistent results, however, are obtained by varying r between 0.8 and 1 according to the indicated temperature gradient:

$$\left.\begin{aligned} &r(\text{Min})=0.8 \quad \text{for} \quad \partial\theta/\partial z\geqslant 10^{-2}\ \text{C m}^{-1}\\ &r(\text{Max})=1 \quad \text{for} \quad \partial\theta/\partial z=0\\ &\lambda=27\text{m}\end{aligned}\right\}. \tag{10}$$

To be sure, this specification is arbitrary although there exists some observational evidence which seems to justify this type of procedure.

Reference is made to another excellent investigation of the distribution of the exchange coefficient in a neutrally stratified boundary layer. This particular analysis, due to Lettau (1962), is not as readily extended to account for stable stratification and for this reason is not used in this study.

The evaluation of K_H requires a knowledge of the wind shear components which also depend on stability. The computation of the wind components u and v from the equations of motion is a very difficult task. Therefore, certain simplifying assumptions are necessary to make the analysis feasible. For this reason, it is assumed that the air density (for wind calculations only) and the geostrophic wind are constant with height and time throughout the boundary layer, and that advection effects can be disregarded.

The equations of horizontal mean motion can now be written as

$$\frac{\partial u}{\partial t}=f(v-v_g)+\frac{\partial}{\partial z}\left(K_m\frac{\partial u}{\partial z}\right), \tag{11a}$$

$$\frac{\partial v}{\partial t}=-f(u-u_g)+\frac{\partial}{\partial z}\left(K_m\frac{\partial v}{\partial z}\right). \tag{11b}$$

These equations are integrated with the boundary conditions that

$$\left.\begin{aligned} &z=z_0 \quad \text{for} \quad u=v=0\\ &z=\infty \quad \text{for} \quad u=u_g,\ v=v_g=0,\ K_m=0\end{aligned}\right\}. \tag{11c}$$

The initial conditions which are necessary to evaluate (11) are discussed in the next section.

d. Determination of initial conditions

In order to evaluate Eqs. (11a) and (11b), reliable initial conditions must be known. Generally, it is impossible to specify u, v and their time derivatives such as to satisfy the equations of motion. This is due to the complicated interrelationships among u, v and K_m. By assuming that initially the air motion is in a steady state and that the temperature distribution is adiabatic, Eqs. (11a,b) can be solved for u, v and $K_{m,n}$ using a method outlined by Blackadar (1962). However, the assumption of the adiabatic boundary layer can be removed by retaining $f(\theta)$ in Eq. (9). The numerical solution technique adopted here, which is not described by Blackadar, utilizes his dimensionless form of the equations of motion. The integration procedure devised by the present authors, based upon the Taylor algorithm, checks out Blackadar's computations. A description of the numerical procedure to obtain the initial data is omitted.

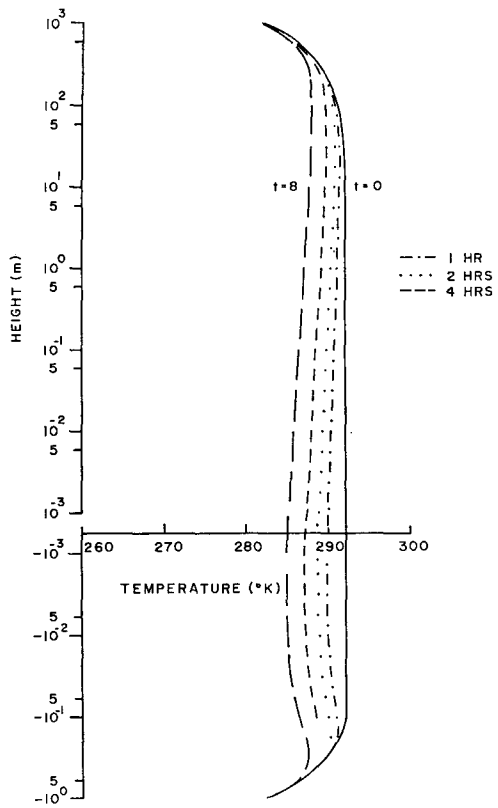

FIG. 1. Air and soil temperature distribution for rocky soil.

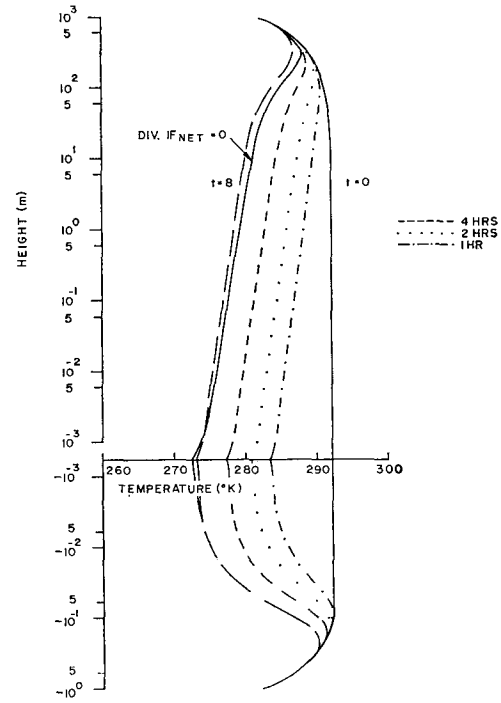

FIG. 2. Air and soil temperature distribution for quartz sand.

3. Discussion of results

a. General remarks

The present analysis requires a specification of soil data. For this purpose, the material constants of four representative soil types are listed next. The data are taken from *Linkes Meteorologisches Taschenbuch.*

Soil type	ρ_s (gm cm^{-3})	C_s [cal gm^{-1} (°C)$^{-1}$]	K_s (cm^2 sec^{-1})
Rocky soil	2.60	0.20	0.0210
Quartz sand	1.65	0.19	0.0020
Sandy clay (15% moisture)	1.78	0.33	0.0037
Humus	1.30	0.44	0.0050

Computations based upon these four soil types are discussed in detail. The initial temperature distribution used in this study is the same in all cases in order to facilitate the discussion. For heights >1 km, the U. S. Standard Atmosphere is chosen; below 1 km the atmosphere is assumed to be adiabatically stratified (in harmony with the discussion of Section 2d,) giving a surface temperature of 19C. The initial soil temperature in the vicinity of the earth's surface is taken constant and then decreased with depth to a value of 9C at 1 m below the surface as indicated in all pertinent figures. The temperature distribution below 1 m is not affected for a computational period of one night.

The moisture distribution, as required for radiation calculations, corresponds to a relative humidity of ~60% for the boundary layer. Above this layer the relative humidity is assumed to decrease slightly with height. Changes in the distribution of moisture due to exchange processes are not considered. Test computations indicate that the optical path lengths of water vapor will be changed only insignificantly due to the absence of sources and sinks. The inclusion of moisture computations, however, increases computer time very strongly.

All computations pertain to a roughness height of 1 cm (short grass) and a latitude of 45N.

b. Temperature predictions for various soil types

In order to evaluate the heat conduction equations, the distribution of the exchange coefficients must be known throughout space. The equations of motion do not furnish the exchange coefficient for heights less than the roughness height of vegetation. Hence, for smaller heights, one must rely on extrapolations. At the surface of the earth, on a calm night, the exchange coefficient of the air cannot differ very strongly from the molecular diffusion coefficient. Therefore, it appears reasonable to extrapolate linearly the exchange coefficient from the roughness height to its minimum value, the molecular diffusion coefficient, at the earth's surface. Figs. 1–4 are obtained on this basis. The consequences of this assumption are discussed later on by using different extrapolations.

It is of interest to note that the computed exchange coefficients at 10 and 200 cm agree well with those obtained by Möller (1955) using an entirely different procedure and the nocturnal average value at 2 m given by Fritzsche and Stange (1936) as quoted by Philipps (1940).

The strongest cooling is observed in conjunction with quartz sand due to the rather poor soil conductivity and the moderately small heat capacity. Sandy clay and humus show a very similar behavior. Above a height of 800 m and below a depth of 1 m, the original temperature sounding remains almost unaffected.

The effect of radiative temperature changes upon the nocturnal temperature profile is not well understood. Möller (1955) states that near the ground this effect is entirely negligible, a conclusion challenged by Gaevskaya *et al.* (1962). The latter authors make the simplifying assumption that the radiative flux divergence, resulting in cooling everywhere, is constant throughout the prediction period. Assuming that the atmosphere is initially isothermally stratified, the same authors find within the lower 5m, that, the combined action of turbulent and radiative cooling is less than the effect of turbulent cooling alone. This is indeed a strange result and may be due to a large extent to the simplifying assumption that the flux divergence does not change with time. Figs. 2 and 3 indicate clearly, although based on different initial conditions not too far removed from isothermal stratification near the ground, that the total effect of the two cooling processes is stronger cooling than the effect of turbulent cooling by itself. The maximum net effect of radiative flux divergence can be as strong as 20% of the total cooling rate. An exception exists for the air directly overlying the ground, in the case of quartz sand. Due to the strong temperature inversion near the earth's surface, one obtains radiative heating near the ground as repeatedly demonstrated in the literature by Fleagle (1953), Möller (1955), Zdunkowski and Johnson (1965) and Zdunkowski *et al.* (1966). This radiative heating is responsible for the fact that the cooling resulting from the combined process is a little smaller than that due to turbulent action alone.

For a fairly steep ground inversion, the radiative temperature change of the air overlying the ground can easily exceed an *instantaneous* value of 10C hr^{-1}. At a height of 80 cm, a temperature change as large as -10C hr^{-1} may be observed. The corresponding temperature changes due to turbulent heat exchange alone amount to -8C hr^{-1} at most as in the case of quartz sand. The small net effect due to radiation indeed leads to the conclusion that the effect of turbulence far outweighs the radiative effect, but not to the extent that the radiative flux divergence is entirely negligible.

Of special interest are the temperature changes at the earth's surface and at the height of the thermograph (here as 180 cm). Results taking into account the effects of radiative flux divergence are depicted in Figs. 5 and 6.

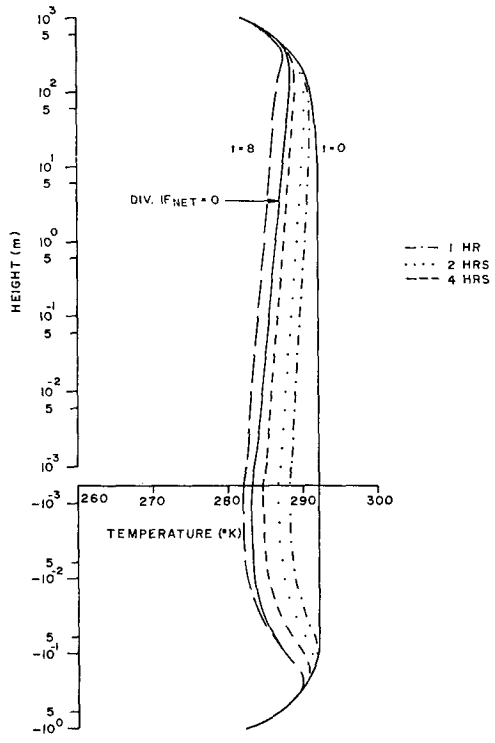

FIG. 3. Air and soil temperature distribution for sandy clay.

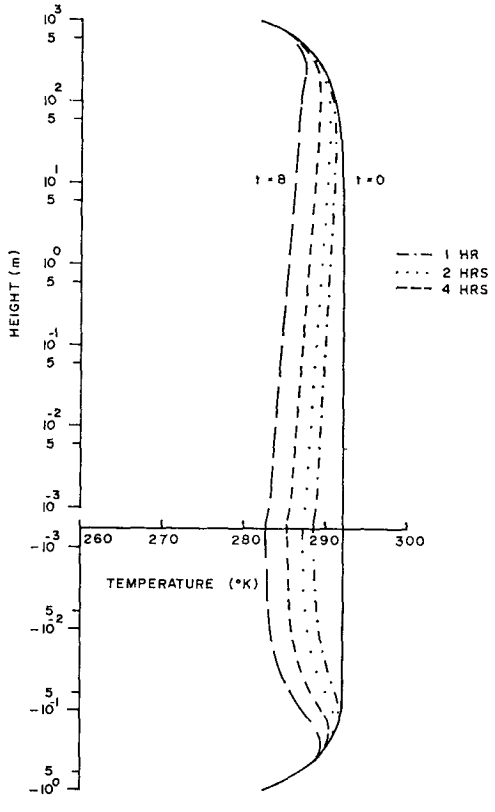

FIG. 4. Air and soil temperature distribution for humus.

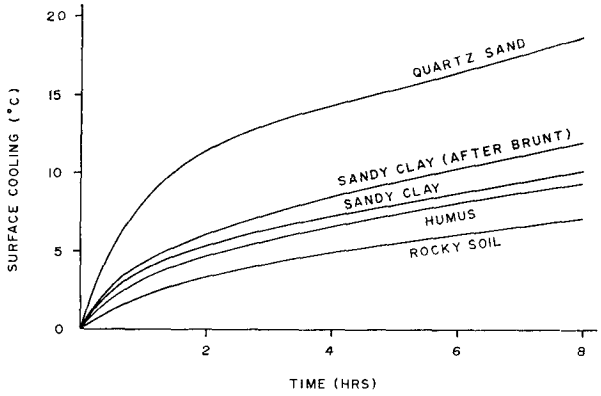

FIG. 5. Surface cooling for different types of soil.

Strongest and weakest cooling are obtained for quartz sand and rocky soil, respectively. Even at the height of the thermograph the temperature change is most critically affected by the underlying soil, amounting to 70% of the surface cooling at the end of the night. While sandy soils may cause ground frost and even endanger fruit trees and plants, loamy and rocky soils remain protected. These facts have important agricultural consequences.

For comparison, in case of sandy clay, the surface cooling computed from Brunt's formula is also included. Due to Brunt's assumption that radiative heat losses from the earth's surface are solely replaced by heat conduction of the soil, the total cooling rate is overestimated by 2C.

Fig. 7 gives inversion heights as a function of time for different soil types. The quickest growth is found for quartz sand. The results seem to be in harmony with observations. Unfortunately, no suitable observational material seems to be available for detailed comparisons.

Figs. 1 through 7 are based on the assumption that the exchange coefficient of the air at the surface of the earth equals the molecular diffusion coefficient. This assumption, to be sure, is arbitrary and must be examined more closely. Möller (1955), on the basis of some observational material for the early morning hours of a calm night, obtains an exchange coefficient for $z=0$ which exceeds the molecular diffusion coefficient by one order of magnitude. Since the observational material was not sufficient for the calculation, Möller had to rely on various extrapolations so that his result may not be accurate.

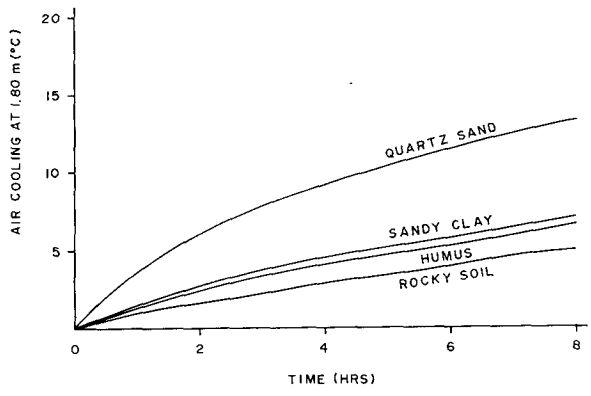

FIG. 6. Air cooling at thermograph height for different types of soil.

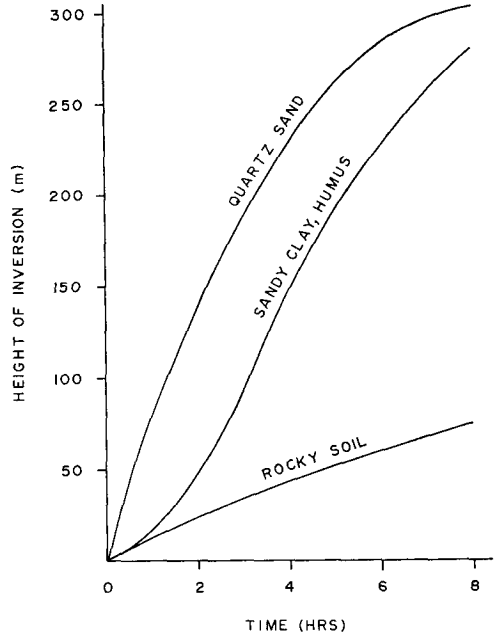

FIG. 7. Inversion heights for different types of soil.

Möller's result, together with a linear variation of the exchange coefficient below the roughness level and a soil type of sandy clay for the entire night, gives a temperature change at $z=0$ and $z=1.80$ m of only 5C and 4C, respectively, roughly one-half the value obtained previously. A value three times as large as Möller's K_H at $z=0$ gives approximately the same result. From this test one is tempted to conclude that Möller's proposed value of the exchange coefficient is too large.

In order to study the influence of K_H at $z=0$, the coefficient is systematically increased. In the interval ranging from 1–3 times the molecular value, the surface temperature change remains virtually unaffected. Next, the exchange coefficient at the ground is increased from 3–7 times its molecular value. Instead of an expected decrease of the surface temperature change of $\sim 20\%$, the temperature change is increased uniformly $\sim 15\%$. Increasing the exchange coefficient from 7–10 times the molecular value results in a uniform temperature decrease to give the previously computed value using Möller's value for $z=0$. This peculiar result should not be withheld. The temperature change distribution above the surface decreases with height for any assumed exchange coefficient and does not show any peculiarities.

A careful analysis reveals that the computations are particularly sensitive in the anomalous region to the type of extrapolation which is used. Extrapolating the exchange coefficient to the same surface value in a different manner is capable of removing this anomaly. Such a procedure proves to be very arbitrary. Therefore, one must conclude that for very accurate computations not only the magnitude of the exchange coefficient at $z=0$ must be well known but also its vertical gradient. Most consistent results, apparently in harmony with observations, are obtained if the exchange coefficient at $z=0$ has a value close to that of the molecular diffusion coefficient. Linear extrapolations seem to be sufficient. (It seems hopeless to accurately determine the exchange coefficient at $z=0$ by reproducing the observed nocturnal temperature profile.)

c. The distribution of the exchange coefficient as a function of height and time

Before the entire analysis becomes feasible, the distribution of the exchange coefficient for neutral conditions must be known. Computational results are shown in Figs. 8 and 9 and are labeled as $t=0$. A small distance below 1000 m it is found that the exchange coefficient suddenly stops decreasing with height and instead starts increasing in value. This is a numerical but not a physical result already experienced by Blackadar (1962). For this reason $K_{m,n}$ is extrapolated to a value of zero which is found to occur at 1000 m. With this new modified distribution, the velocity components u, v are recomputed to furnish the initial data which are required to solve the equations of motion for the non-steady-state situation.

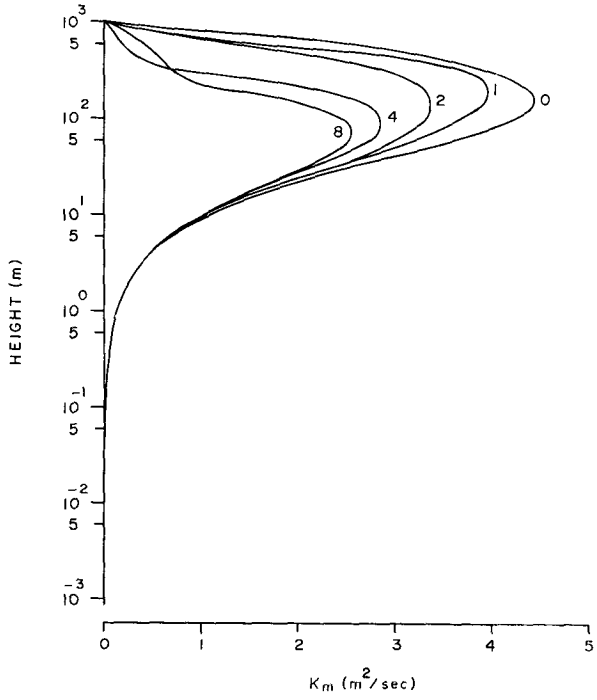

FIG. 8. Distribution of exchange coefficients over rocky soil.

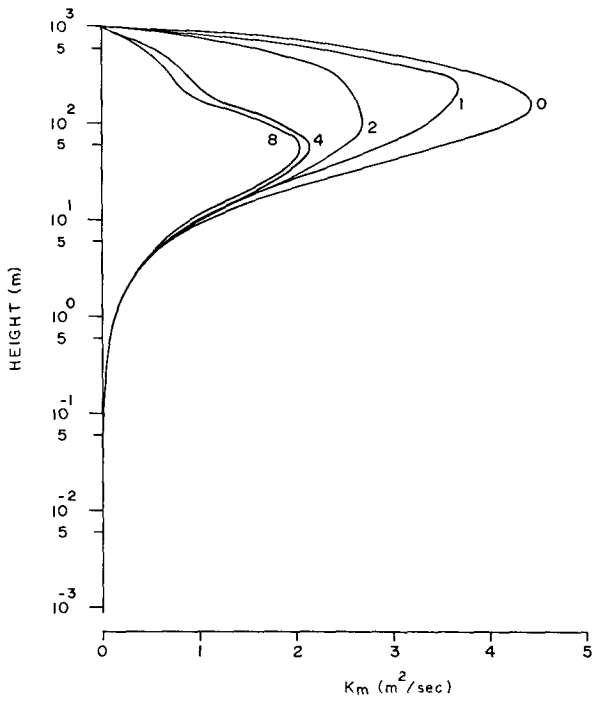

FIG. 9. Distribution of exchange coefficients over sandy clay.

The distribution of the exchange coefficient as a function of time is discussed next. Two samples, corresponding to Figs. 1 and 3, are shown in Figs. 8 and 9. The distribution of the remaining types is similar and is not reproduced here. In general, after the time of sundown, the exchange coefficients diminish in magnitude. The maximum values decrease to approximately one-half their original magnitude. At the same time, the heights of the maximum values decrease.

For greater clarity, these results are depicted in Figs. 10 and 11 for all four soil types studied here. As will be seen, the maximum values as well as the corresponding heights decrease with stability in a fairly regular fashion. An exception is due to quartz sand which is explained in terms of the rapid surface cooling as well as the fairly strong interaction of radiative and turbulent heat exchange. For comparison, in the case of quartz sand, the artificial case is shown which also assumes that the radiative flux divergence is absent. Inspection of Fig. 10 makes it clear that radiation is partly responsible for the anomaly.

This result is somewhat paralleled in Fig. 11. It is remarkable in the particular case of quartz sand, where very strong desert type cooling occurs, that the height of the maximum exchange coefficient rises within the first hour from 185 to 315 m. After another hour, this particular height decreases rapidly to a height of 40 m where it remains for the rest of the night. This peculiar

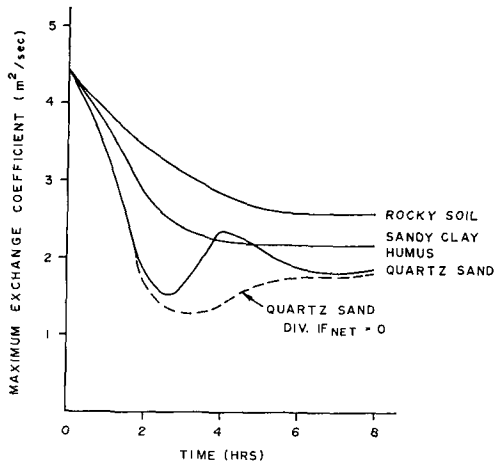

FIG. 10. Distribution of maximum exchange coefficients for various types of soil.

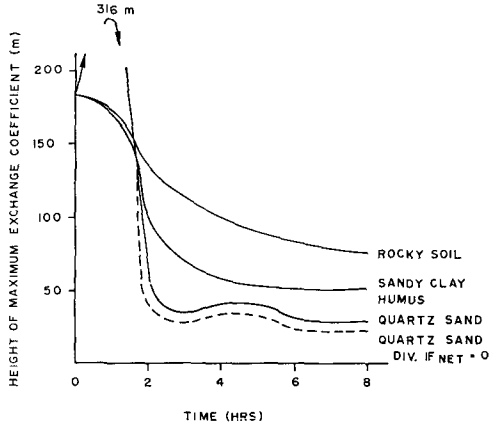

FIG. 11. Heights of maximum exchange coefficients for various types of soil.

result can be explained only by assuming that within the first hour, the period of maximum surface and air cooling, the atmosphere is far removed from the initially imposed steady-state conditions. For this reason, a rapid adjustment is taking place.

A further inspection of Figs. 8 and 9 indicates that within the lower 10 m the effect of thermal stability upon the exchange coefficient is very slight. The large effect of the velocity shear in Eq. (9) outweighs by far the contribution of the temperature gradient. In nature, one also expects in low levels a decrease of the exchange coefficient with time. Nevertheless, in the height interval from 10 to 50 cm the computed exchange coefficients are in good agreement with those obtained from Möller which presumably represent the second half of a calm night. For greater heights (50–80 m) good agreement is also found with the nocturnal mean values given by Fritzsche and Stange as reported by Lettau (1939). For the layer in between, the exchange coefficients represented here increase more rapidly than those of the mentioned authors.

d. The distribution of wind velocities in the boundary layer

The wind spirals corresponding to Figs. 1, 2 and 3 are shown in Figs. 12, 13 and 14. The distribution of wind with respect to soil type humus is omitted since it is not sufficiently different from Fig. 14.

The numbers in parentheses referring to points on the wind spiral give the wind velocities at certain heights. Referring to Fig. 12, for example, wind vectors drawn from the origin to the points labeled (316) for $t=0$ (time of sundown) and $t=8$ (end of the prediction period) correspond to velocities of 10.13 and 11.05 m sec^{-1}, respectively, at a height of 316 m.

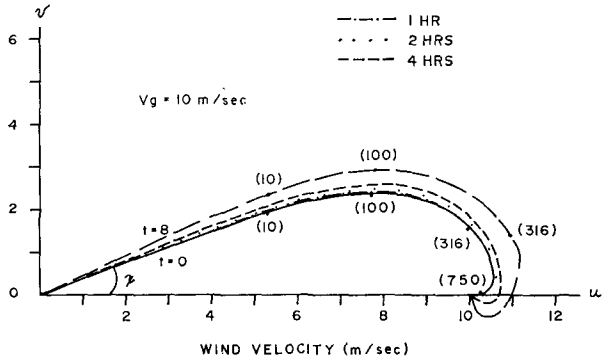

FIG. 12. Wind spirals for rocky soil.

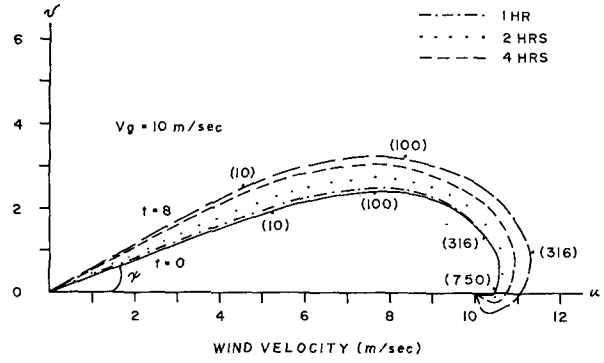

FIG. 13. Wind spirals for quartz sand.

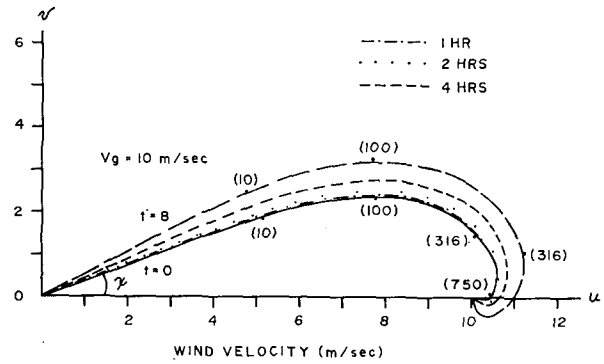

FIG. 14. Wind spirals for sandy clay.

The similarity of the wind spirals presented here with the Ekman solution is evident. The wind vectors spiral around the maximum value of the u component and finally approach the geostrophic wind (10 m sec^{-1}, $\psi=0°$). Neglecting the flux divergence of radiation in the calculations results in only very minor changes of the spirals which are not shown.

The behavior of the wind spirals, at least qualitatively, satisfies the requirements of observation and theory. At smaller heights the wind velocities generally decrease slightly with increasing stability, and increase with increasing stability at greater heights. The degree of change depends on the soil type and is more strongly pronounced in the case of quartz sand.

The cross-isobar angle decreases with height for each particular time. Variations of the surface cross-isobar angle, determined by the surface and geostrophic wind direction, are shown in Fig. 15. The large increase is associated with strongest cooling of the air as evidenced by soil type quartz sand. The value of the cross-isobar angle of 30° is in good agreement with an estimate of Frost (1948).

Finally, the variation of the gradient wind height with time, i.e., with increasing stability, is considered. Results are shown in Fig. 16. From its initial value of 750 m in the steady-state case of the neutral atmosphere, the gradient wind level is decreasing uniformly with time. A strong variation of the gradient wind heights as a function of soil data is not observed. This result is somewhat surprising. The final height of ~500 m is in good agreement with an estimate made by Haltiner and Martin (1957).

4. Concluding remarks

Results obtained from this analysis indicate very clearly the possibility of predicting nocturnal temperature profiles on a numerical basis. Realistic results are obtained for all cases studied. The entire analysis is based upon theoretical grounds using empirical data only very sparingly. The nonlinear character of the basic equations makes it very difficult, perhaps impossible, to give analytic statements on the accuracy of the computations. Increasing the density of grid points results in changes which are only very insignificant. The computational scheme, as applied to the case for which analytic solutions are available, gives very satisfactory agreement.

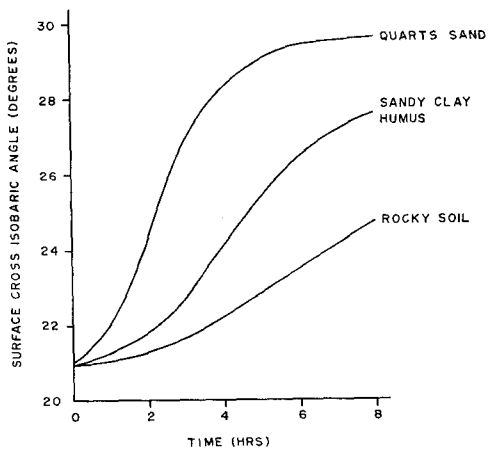

FIG. 15. Surface cross isobar angles for various types of soil.

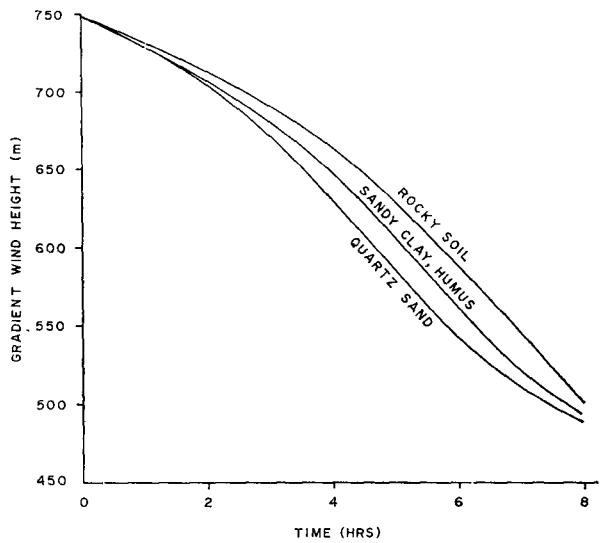

FIG. 16. Gradient wind heights for various types of soil.

In the future, the analysis can be improved by including the effects of advection and by permitting the geostrophic wind to increase with height. The inclusion of the moisture transport equations in the present analysis would make it possible to predict radiation fog and its vertical growth along the lines proposed by Zdunkowski aad Nielsen (1969).

Wu (1965), disregarding radiative effects, also predicts the temperature profile using a slightly modified form of Eq. (9). Instead of computing the shear terms of the wind velocity, she uses measured data which makes it possible to compare predicted and observed temperature profiles. Wu obtains reasonable results by adjusting the parameter λ to account for stability effects.

Acknowledgments. The research was sponsored by the U. S. Army Electronic Command, Atmospheric Sciences Laboratory, Fort Huachuca, Ariz. Gratitude is expressed to Prof. Jan Paegle, University of Utah, for helpful discussions of the manuscript.

APPENDIX A

List of Symbols

T,θ,T_s temperature and potential temperature of the air, soil temperature

z,z_0,t	height coordinate, roughness height, time
K_m,K_H	exchange coefficients of air for momentum and heat flux
K_s	exchange coefficient for molecular conduction of the soil
ρ,ρ_s	density of air and soil.
c_p,c_s	specific heat constant of air at constant pressure, and of the soil
F_N	net flux of radiation
B	Stefan-Boltzmann function
τ	transmission function
w,W	optical pathlength of water vapor, total atmospheric value
k,l	von Kármán's constant and mixing length.
u,v	components of the wind velocity along x and y axes.
u_g,v_g	components of the geostrophic wind
f	Coriolis parameter
g	acceleration of gravity
p	air pressure

APPENDIX B

1. Solution of the heat conduction equation

Let α represent a scalar quantity. The heat conduction equation is now of the general form

$$\frac{\partial\alpha}{\partial t}=\frac{\partial K}{\partial z}\frac{\partial\alpha}{\partial z}+K\frac{\partial^2\alpha}{\partial z^2}. \tag{1b}$$

By expressing α in terms of a Taylor series, one may obtain for level i the following finite-difference equations for the first and second derivatives (for details see Zdunkowski and Nielsen, 1969):

$$\left(\frac{\partial^2\alpha}{\partial z^2}\right)_i=2\frac{[\Delta z_i\alpha_{i-1}-(\Delta z_{i-1}+\Delta z_i)\alpha_i+\Delta z_{i-1}\alpha_{i+1}]}{\Delta z_{i-1}\Delta z_i(\Delta z_{i-1}+\Delta z_i)}$$
$$+O(\Delta z_i-\Delta z_{i-1})+O(\Delta z_i^2), \tag{2b}$$

where $\Delta z_i=z_{i+1}-z_i$ and

$$\left(\frac{\partial\alpha}{\partial z}\right)_i=-\frac{\Delta z_i^2\alpha_{i-1}-(\Delta z_{i-1}^2-\Delta z_i^2)\alpha_i+\Delta z_{i-1}^2\alpha_{i+1}}{\Delta z_{i-1}\Delta z_i(\Delta z_{i-1}+\Delta z_i)}$$
$$+O(\Delta z_i^2). \tag{3b}$$

The quantity $(\partial k/\partial z)$ is expressed analogously. The error terms are due to discretization.

Since $O(\Delta z_i-\Delta z_{i-1})\approx O(\Delta z_i^2)$, both equations are considered to be second-order approximations to the derivatives.

The computations of the exchange coefficient requires a knowledge of $\partial\theta/\partial z$, $\partial u/\partial z$ and $\partial v/\partial z$. The previously defined finite-difference scheme, as given by Eq. (3b), is usable for this purpose with the exception of the boundary points [i.e., $(\partial\theta/\partial z)_{z=0}$ and $(\partial(u,v)/\partial z)_{z=z_0}$]. Here it is necessary to use a forward-difference formula. Since the approximation to the derivatives everywhere else is of a second order, it is desirable to have a corresponding approximation; the result is

$$\left(\frac{\partial\alpha}{\partial z}\right)_i=\frac{-\Delta z_{i+1}(2\Delta z_i+\Delta z_{i+1})\alpha_i+(\Delta z_{i+1}+\Delta z_i)^2\alpha_{i+1}-\Delta z_i^2\alpha_{i+2}}{\Delta z_i\Delta z_{i+1}(\Delta z_i+\Delta z_{i+1})}. \tag{4b}$$

Here Δz_i represents the height increment between the boundary surface and the first selected level.

Let the superscript j represent the time grid. In finite-difference form the heat conduction equation can be written in its most simple form as

$$\frac{\alpha_i^{j+1}-\alpha_i^j}{\Delta t}=\delta K_i^j\delta\alpha_i^j+K_i^j\delta^2\alpha_i^j, \tag{5b}$$

where $\delta\alpha\approx\partial\alpha/\partial z$ and $\delta^2\alpha\approx\partial^2\alpha/\partial z^2$. This is an explicit equation since α_i^{j+1} is the only unknown quantity. In order to have a computationally stable finite-difference scheme, an implicit finite-difference scheme must be used. This can be expressed (Richtmeyer and Morton, 1967) as

$$\frac{\alpha_i^{j+1}-\alpha_i^j}{\Delta t}=\gamma(\delta K_i^{j+1}\delta\alpha_i^{j+1}+K_i^{j+1}\delta^2\alpha_i^{j+1})$$
$$+(1-\gamma)(\delta K_i^j\delta\alpha_i^j+K_i^j\delta^2\alpha_i^j),\quad 0<\gamma\leqslant 1. \tag{6b}$$

Choosing $\gamma=1$ the above equation is completely implicit. However, this formula cannot be used since the exchange coefficient is a nonlinear function of the potential temperature. It is therefore necessary to evaluate K at time j.

If Δz_{sfc} and $\Delta z_{\text{sfc}-1}$ stand for height increments directly above and below $z=0$, respectively, the distribution of α at the surface (see Zdunkowski and Nielsen, 1969) is given by

$$\frac{\alpha_{\text{sfc}}^{j+1}-\alpha_{\text{sfc}}^j}{\Delta t}$$
$$=\left(\frac{c_pK_{H,\text{sfc}}\rho\Delta z_{\text{sfc}}}{K_{H,\text{sfc}+1}-3K_{H,\text{sfc}}}-\frac{c_sK_{s,\text{sfc}}\rho_s(z=0)\Delta z_{\text{sfc}-1}}{3K_{s,\text{sfc}}-K_{s,\text{sfc}-1}}\right)^{-j}$$
$$\times\left\{F_N(z=0)+\left[\frac{2c_p\rho K_{H,\text{sfc}}^2}{\Delta z_{\text{sfc}}(K_{H,\text{sfc}+1}-3K_{H,\text{sfc}})}\right]^j\right.$$
$$\times(\alpha_{\text{sfc}+1}^{j+1}-\alpha_{\text{sfc}}^{j+1})-\left[\frac{2c_s\rho_s(z=0)K_{s,\text{sfc}}^2}{\Delta z_{\text{sfc}-1}(3K_{s,\text{sfc}}-K_{s,\text{sfc}-1})}\right]^j$$
$$\left.\times(\alpha_{\text{sfc}+1}^{j+1}-\alpha_{\text{sfc}}^{j+1})\right\}. \tag{7b}$$

2. Solution of equations of motion

The equations of motion as given by (11a,b) in finite difference are of the form

$$\frac{u_i^{j+1}-u_i^j}{\Delta t}=f(v_i^{j+1}-v_g)$$
$$+2K_i^j\left[\frac{\Delta z_i u_{i-1}^{j+1}-(\Delta z_{i-1}+\Delta z_i)u_i^{j+1}+\Delta z_{i-1}u_{i+1}^{j+1}}{\Delta z_{i-1}\Delta z_i(\Delta z_{i-1}+\Delta z_i)}\right]$$
$$+\left[\frac{-\Delta z_i^2 K_{i-1}^j-(\Delta z_{i-1}^2-\Delta z_i^2)K_i^j+\Delta z_{i-1}^2 K_{i+1}^j}{\Delta z_{i-1}\Delta z_i(\Delta z_{i-1}+\Delta z_i)}\right]$$
$$\times\left[\frac{-\Delta z_i^2 u_{i-1}^{j+1}-(\Delta z_{i-1}^2-\Delta z_i^2)u_i^{j+1}+\Delta z_{i-1}^2 u_{i+1}^{j+1}}{\Delta z_{i-1}\Delta z_i(\Delta z_{i-1}+\Delta z_i)}\right]. \tag{8b}$$

A similar expression is valid for the v component. As will be seen, the velocity is expressed completely implicity, while K, because of nonlinearity, is expressed explicitly.

A rearrangement of the finite difference scheme permits one to write the equations of motion in the general form

$$\left.\begin{aligned}Au_{i-1}^{j+1}+Bu_i^{j+1}+Cu_{i+1}^{j+1}+Dv_i^{j+1}=F\\ Gv_{i-1}^{j+1}+Hv_i^{j+1}+Iv_{i+1}^{j+1}+Ju_i^{j+1}=K\end{aligned}\right\}. \tag{9b}$$

The constants, of course, are functions of height. In order to solve the equations of motion, Eq. (9b) is written for each level. The solution of the u,v, components is affected by the Gaussian elimination scheme.

In order to insure computational stability, time integrations are carried out over steps of 50 sec. Using time steps somewhat larger or considerably less give highly consistent results.

3. Stability analysis

Let $u'=u-u_g$ and $v'=v-v_g$. By multiplying the v component of the equations of motion by $\sqrt{-1}=i'$ and adding it to the u component, i.e., $W=u'+iv'$, one obtains

$$\frac{\partial W}{\partial t}+i'fW-K\frac{\partial^2 W}{\partial z^2}-\frac{\partial K}{\partial z}\frac{\partial W}{\partial z}=0. \tag{10b}$$

In finite differences, it is evaluated in the form

$$\frac{W_i^{j+1}-W_i^j}{\Delta t}\approx -i'fW_i^{j+1}$$
$$+K_i^j\frac{\partial^2 W_i^{j+1}}{\partial z^2}+\frac{\partial K_i^j}{\partial z}\frac{\partial W_i^{j+1}}{\partial z}. \tag{11b}$$

Momentarily, we consider only the first term of the right-hand side of (11b), giving the solution A exp $(-i'ft)$, where A is a constant. It should be pointed out, however, that the (11b) approximation for this term does give rise to a slight numerical instability for small enough time steps. If integration steps in time are taken as $\Delta t=50$ sec, then for the prediction period of 8 hr an amplification (dampening) error of approximately 0.7% is caused which is certainly of smaller magnitude than errors introduced by various assumptions. We next consider only the second term of the right-hand side of (11b). For constant K, the numerical scheme, as previously outlined, is always stable (Richtmyer and Morton, 1967). Considering now the third term, particularly near the ground, we note that the exchange coefficient changes linearly with height so that $\partial K/\partial z$ is constant and locally nearly constant elsewhere for the considered height intervals; thus, the implicit treatment should make this term stable also. Hence, it can be expected that the entire finite-difference scheme represents a fairly stable system.

In order to keep the Coriolis term reasonably stable, all computations are carried out for time increments of 50 sec although time steps considerably smaller and somewhat larger give highly consistent results. The following heights are normally used in the computations: $z=-1.00$, -0.75, -0.56, -0.42, -0.31, -0.24, -0.17, -0.13, -0.1, -0.075, ..., -0.0075, ..., -0.001, 0, 0.001, 0.0013, 0.0018, 0.0024, 0.0032, 0.0042, 0.0056, 0.0075, 0.01, 0.013, ..., 13000 m.

Using a somewhat smaller or larger number of height intervals again gives highly consistent results.

After a period of 4–6 hr, very slight oscillations in time become noticeable. These are completely suppressed by a simple time average of the exchange coefficient according to

$$K_{m,i}^j=\tfrac{1}{4}(K_{m,i}^j+2K_{m,i}^{j-1}+K_{m,i}^{j-2}).$$

For a period of 4 hr, only very insignificant differences in results for smoothed and non-smoothed exchange coefficients could be detected. This seems to justify the adoption of the smoothing procedure.

REFERENCES

Blackadar, Alfred K., 1962: The vertical distribution of wind and turbulent exchange in a neutral atmosphere. *J. Geophys. Res.*, **67**, 3095–3102.

Brunt, D., 1940: Radiation in the atmosphere. *Quart. J. Roy. Meteor. Soc.*, **66**, Supplement, 34–40.

Estoque, M. A., 1963: A numerical model of the atmospheric boundary layer. *J. Geophys. Res.*, **86**, 1103–1113.

Fleagle, R. C., 1953: A theory of fog formation. *J. Marine Res.*, **12**, 43–50.

Fritzsche, G. and R. Stange, 1936: Vertikaler Temperaturverlauf über einer Grosstadt. *Beitr. Phys. Atmos.*, **23**, 95–100.

Frost, R., 1948: Atmospheric turbulence. *Quart. J. Roy. Meteor. Soc.*, **74**, 316–338.

Gaevskaya, G. N., K. Y. Kondrati'ev and K. E. Yakuschevskaya, 1962: Radiative heat flux divergence and heat regime in the lowest layer or the atmosphere. *Arch. Meteor.*, **12**, 95–108.

Haltiner, George J., and Frank L. Martin, 1957: *Dynamical and Physical Meteorology*. New York, McGraw-Hill, 240–248.

Heisenberg, W., 1948: Zur statistischen Theorie der Turbulenz. *Z. Phys.* **124**, 628–657.

Jaeger, J. C., 1945: Note of the effect of wind on nocturnal cooling *Quart. J. Roy. Meteor. Soc.*, **71**, 388–390.

Knighting E., 1950: A note on nocturnal cooling. *Quart. J. Roy. Meteor. Soc.*, **76**, 173–181.

Kuhn, J. V., 1963: Radiometersonde observations of infrared flux emissivity of water vapor. *J. Appl. Meteor.*, **2**, 368–378.

Kuo, H. L., 1968: The thermal interaction between the atmosphere and the earth and propagation of diurnal temperature waves. *J. Atmos. Sci.*, **25**, 682–706.

Lettau, Heinz, 1939: *Atmosphärische Turbulenz*. Leipzig, Akad. Verlagsgesellschaft, 133–141.

——, 1962: Theoretical wind spirals in the boundary layer of a barotropic atmosphere. *Beitr. Phys. Atmos.*, **35**, 195–212.

Möller, Fritz, 1943: Das Strahlungsdiagramm. *Wiss. Abhandl. Deut. Reiches Wetterdienst.*

——, 1955: Strahlungsvorgänge in Bodennähe. *Z. Meteor.*, **9**, 47–53.

Pandolfo, J. P., Cooley, D. S. and Atwater, M. A., 1964: Further investigations of numerical models of the atmosphere boundary layer. Tech. Rept., The Travelers Research Center, Inc., Hartford, Conn.

——, —— and ——, 1965: The development of a numerical prediction model for the planetary boundary layer. The Travelers Research Center, Inc., Hartford, Conn.

Philipps, H., 1940: Die nächtliche Abkühlung des Erdbodens durch Strahlung und Wärmeleitung und der Bodenschicht durch Turbulenz. *Beitr. Geophys.*, **56**, 23 pp.

——, 1962: Zur Theorie des Tagesganges der Temperatur in der bodennahen Atmosphäre und in ihrer Unterlage. *Z. Meteor.*, **16**, 5–46.

Richtmyer, Robert D., and K. W. Morton, 1967: *Difference Methods for Initial-Value Problems*. New York, Interscience, 403 pp.

Wu, Sharon S., 1965: A study of heat transfer coefficients in the lowest 400 meters of the atmosphere. *J. Geophys. Res.*, **70**, 1801–1808.

Zdunkowski, W. G., and F. E. Johnson, 1965: Infrared flux divergence calculations with newly constructed radiation tables. *J. Appl. Meteor.*, **4**, 371–377.

——, D. Henderson, and J. V. Hales, 1966: The effect of atmospheric haze on infrared radiative cooling rates. *J. Atmos. Sci.*, **23**, 297–304.

——, —— and ——, 1967: Prediction of nocturnal temperature changes during a calm night. *Beitr. Phys. Atmos.*, **40**, 144–157.

——, and Nielsen, B. C., 1969: A preliminary prediction analysis of radiation fog. *Pure Appl. Geophys.*, **75**, 278–299.